Article

Journal of Vibration and Control
1–12

DOI: 10.1177/1077546315616699
jvc.sagepub.com
SAGE

Dependent modal space control: Experimental test rig

Mattia Serra[1], Ferruccio Resta[2] and Francesco Ripamonti[2]

Abstract

This article presents the experimental validation of a new control technique for reducing vibration in flexible structures: Dependent modal space control. While the classic independent modal space control allows only the frequency and the damping of the controlled modes to be changed, dependent modal space control can also impose the controlled mode shapes. Depending on the kind and number of sensors and actuators available for control, the mode shape can be imposed in both a direct and an indirect way. Owing to the need for modal sensors and actuators for direct mode shape imposition, the second methodology is often preferred in many engineering applications. In the indirect method, the optimal closed loop mode shapes set is computed with an optimization algorithm in order to minimize an Input-Output Performance Index. The worsening spillover effects due to errors in the estimates of the system state variables are considered when computing the gain matrix and play an important role in the entire control logic. Experimental validation on a cantilevered beam shows the effectiveness of the dependent modal space control and a good match between the numerical and the experimental results.

Keywords

Eigenstructure assignment, independent modal space control, optimal control, experimental validation, flexible structures

1. Introduction

Over the past decade much research has been done on reducing vibrations in flexible structures. Most of this work focused on feedback control of large flexible systems at relatively low frequencies. This is because light and flexible structures generally have low damping ratios, especially on the first modes, which in many applications are also those most excited. Vibrations cause many problems ranging from fatigue issues to noise, or simply downgrade system performance by exceeding the acceptable thresholds in precision applications.

Among the different strategies for vibration control, one of the best known is modal control, introduced by Balas (1978) and Meirovitch et al. (1983) between the 70s and 2000. It is a model-based logic that permits control of continuum structures, with infinite degrees of freedom (dof), through a reduced order model in principal coordinates. Furthermore, unlike many other control logics, modal control has a well-defined physical meaning in the gain matrix definition. In the 80s, Meirovitch proposed the Independent Modal Space Control (IMSC), introducing a modal filter to estimate the modal states needed by the controller (Meirovitch and Baruh, 1985).

Starting from the original IMSC, many variants have been developed in order to increase the performance and reduce the effects of control and observation spillover (see for example, Resta et al. (2010) or Bagordo et al. (2011)). To achieve this, for example Baz and Poh (1990) and later Fang et al. (2003) developed Modified Independent Modal Space Control (MIMSC) using part of the weighting matrices entries of the Linear Quadratic Regulator (LQR) method. A further modification of MIMSC was developed by Singh et al. (2003). In their strategy, the energy of different modes is checked at specific intervals of time and

[1]Institute for Mechanical Systems, ETH Zurich, Switzerland
[2]Mechanical Engineering Department, Politecnico di Milano, Italy

Received: 9 April 2015; accepted: 17 October 2015

Corresponding author:
Francesco Ripamonti, Mechanical Engineering Department, Politecnico di Milano, Milano, Italy.
Emails: francesco.ripamonti@polimi.it; serram@ethz.ch

the greatest part of control effort is always directed towards the dominant modes.

Kim and Inman (2001) developed a sliding mode observer in order to eliminate observation spillover, thus improving the performance of IMSC and ensuring greater robustness in the control method. From a theoretical point of view, all these methods make it possible to independently modify frequencies and damping ratios of the controlled modes without affecting the system mode shapes. This result is achieved through a diagonal gain matrix in principal coordinates.

In addition, other nonmodel based control logics, such as the pole-zero assignment method by Mottershead et al. (2008), have been developed. These generally require co-located sensors and actuators and allow the improvement of selected Frequency Response Functions (FRFs) through zeros and poles placement.

The control logic presented by the authors, Dependent Modal Space Control (DMSC) (Serra et al., 2013), is model-based and modifies both the eigenvalues and the eigenmodes of the controlled system exploiting a full gain matrix in principal coordinates. In other words, in terms of available control parameters, some of the coefficients of the gain matrix are used to assign the closed loop poles, while the remainder are used to impose the corresponding eigenvectors.

The main benefit of this method is improved vibration reduction through mode shape modifications using a suitably defined performance index. Model-based techniques mainly focused on increasing damping ratios, while this approach makes it possible to place the closed loop poles and independently select an optimal set of controlled mode shapes. This improves the robustness and performance of the closed loop system compared with IMSC, where the mode shapes are left unaltered. In the case of distributed sensors-actuators, and thus with no spillover, it is possible, for example, to impose directly the mode shapes creating virtual nodes in desired locations, offering considerable advantages in many engineering applications.

In most control problems, however, only a limited number of actuators and sensors are available and the above result cannot be achieved. For this reason, in an alternative approach, the mode shapes are computed by optimizing a desired performance index. Moreover, the minimization problem can be constrained in order to ensure internal stability of the closed loop system on a set of modes that can be greater than the controlled ones.

This number is a control design question and has to be selected balancing the accuracy of the performance index and the effort required to identify the system's parameters.

Considering the most general condition with discrete sensors and actuators not co-located, an experimental validation is carried out to demonstrate the method's performance on a clamped beam controlled with piezoelectric actuators and accelerometers.

IMSC has been broadly applied to different kinds of mechanical structures ranging from large multi-body systems, where for example hydraulic actuators have been used to feedback the control action (Resta et al., 2010), to light smart structures equipped with piezoelectric or piezoceramic actuators and accelerometers (Balas, 1978; Chandrashekhara and Agarwal, 1993; Fuller et al., 1992; Qiu et al., 2007).

Therefore the aim of this paper is to show the experimental validation of DMSC. Only a brief description of the DMSC theory is given with a focus on the worsening spillover effects and the importance of the state space observer. For a detailed explanation of the gain matrix synthesis of the DMSC control theory the reader is referred to Serra et al. (2013). Then, the identification stage for estimating the modal parameters needed to model the system and synthesize the gain matrices is illustrated. Finally, a comparison is made between the system in open and closed loop, highlighting the improved performance of DMSC with respect to IMSC.

2. The dependent modal space control: Direct and indirect eigenstructure assignment

This section recalls the modal space control formulation and the analytical method used to assign eigenvalues and eigenvectors of a Linear Time Invariant (LTI) system broadly described in Serra et al. (2013). The proposed method has been developed specifically for mechanical systems and thus has some restrictions compared with a more general eigenstructure assignment procedure described for instance in Liu and Patton (1998) or Klein and Moore (1977). The main differences introduced here are due to the state space formulation of the mechanical systems described in modal coordinates, the synthesis of the control strategy in frequency domain and the use of an optimization algorithm.

2.1. Direct eigenstructure assignment

Consider the generic description of a mechanical system

$$\mathbf{M}\ddot{\mathbf{z}} + \mathbf{R}\dot{\mathbf{z}} + \mathbf{K}\mathbf{z} = \mathbf{\Lambda}_{\mathbf{f_c}}^{\mathrm{T}}\mathbf{f_c} + \mathbf{\Lambda}_{\mathbf{f_d}}^{\mathrm{T}}\mathbf{f_d} \tag{1}$$

where $\mathbf{M}$, $\mathbf{R}$, $\mathbf{K}$ are respectively the inertial, damping and stiffness matrices, the vector $\mathbf{z}$ contains the independent variables in physical coordinates, the Jacobian matrices $\mathbf{\Lambda}_{\mathbf{f_c}}^{\mathrm{T}}$ and $\mathbf{\Lambda}_{\mathbf{f_d}}^{\mathrm{T}}$ link the force application points with the independent variables and $\mathbf{f_c}$, $\mathbf{f_d}$ are the control

forces and the disturbance acting on the system. For both discrete and continuous systems, the matrices can be obtained from analytical models, with numerical methods, using for instance the Finite Element Method (FEM), or experimental tests. Also in the case of continuous systems, the modeling provides discrete matrices (n dof) and a model space control technique can be applied. From equation (1), it is possible to rewrite the system in principal coordinates ($\mathbf{q_n}$) through a transformation matrix $\mathbf{\Phi} \in \mathbb{R}^{n \times n}$, containing the eigenvectors of $\mathbf{M^{-1}K}$, or equivalently, the mode shapes of the system. Defining

$$\mathbf{z} = \mathbf{\Phi q_n} \tag{2}$$

the system equations of motion become

$$\mathbf{M_q \ddot{q}_n} + \mathbf{R_q \dot{q}_n} + \mathbf{K_q q_n} = \mathbf{B_{qc} f_c} + \mathbf{B_{qd} f_d} \tag{3}$$

where

$$\begin{aligned} \mathbf{M_q} &= \mathbf{\Phi^T M \Phi} \\ \mathbf{R_q} &= \mathbf{\Phi^T R \Phi} \\ \mathbf{K_q} &= \mathbf{\Phi^T K \Phi} \\ \mathbf{B_{qc}} &= \mathbf{\Phi^T \Lambda_{f_c}^T} \\ \mathbf{B_{qd}} &= \mathbf{\Phi^T \Lambda_{f_d}^T} \end{aligned} \tag{4}$$

In many mechanical systems, the structural damping satisfies the Rayleigh assumption, i.e. $\mathbf{R} = \alpha \mathbf{M} + \beta \mathbf{K}$, with α, $\beta \in \mathbb{R}$, and the transformation matrix $\mathbf{\Phi}$ diagonalizes the matrix differential equation so that each mode evolves independently from the others. This makes it possible to separate the contribution of the m modeled modes and the nm nonmodeled modes

$$\begin{cases} \mathbf{M_{qm} \ddot{q}_m} + \mathbf{R_{qm} \dot{q}_m} + \mathbf{K_{qm} q_m} = \mathbf{B_{qcm} f_c} + \mathbf{B_{qdm} f_d} \\ \mathbf{M_{qnm} \ddot{q}_{nm}} + \mathbf{R_{qnm} \dot{q}_{nm}} + \mathbf{K_{qnm} q_{nm}} = \mathbf{B_{qcnm} f_c} + \mathbf{B_{qdnm} f_d} \end{cases} \tag{5}$$

The selection of the number of modeled modes is determined by the frequency range in which the model has to describe the system dynamics and on further aspects related to the control logic acting on it. Once this parameter is selected, the control gain matrices ($\mathbf{G_v}$ and $\mathbf{G_p}$) are synthesized on the reduced order model considering the m modeled modes

$$\mathbf{f_c} = -\mathbf{B_{qcm}^{-1}} \left(\mathbf{G_v \dot{q}_m} + \mathbf{G_p q_m} \right) \tag{6}$$

leading to the closed loop description of the system

$$\mathbf{M_{qc} \ddot{q}_n} + \mathbf{R_{qc} \dot{q}_n} + \mathbf{K_{qc} q_n} = \mathbf{B_{qd} f_d} \tag{7}$$

where

$$\begin{aligned} \mathbf{M_{qc}} &= \begin{bmatrix} \mathbf{M_{qm}} & \mathbf{[0]} \\ \mathbf{[0]} & \mathbf{M_{qnm}} \end{bmatrix} \\ \mathbf{R_{qc}} &= \begin{bmatrix} \mathbf{R_{qm}} + \mathbf{G_v} & \mathbf{[0]} \\ \mathbf{B_{qcnm} B_{qcm}^{-1} G_v} & \mathbf{R_{qnm}} \end{bmatrix} \\ \mathbf{K_{qc}} &= \begin{bmatrix} \mathbf{K_{qm}} + \mathbf{G_p} & \mathbf{[0]} \\ \mathbf{B_{qcnm} B_{qcm}^{-1} G_p} & \mathbf{K_{qnm}} \end{bmatrix} \\ \mathbf{B_{qd}} &= \begin{bmatrix} \mathbf{B_{qdm}} \\ \mathbf{B_{qdnm}} \end{bmatrix} \end{aligned} \tag{8}$$

This description of the system clearly shows the effect of control spillover in the lower left entries of the matrices $\mathbf{R_{qc}}$ and $\mathbf{K_{qc}}$ coupling the modeled and nonmodeled modes.

The control gain matrices $\mathbf{G_v}$ and $\mathbf{G_p}$ modify the closed loop damping and stiffness matrices for the modeled modes, determining the correspondent poles and mode shapes. While in IMSC these matrices are diagonal, leaving the decoupled nature of the principal coordinates unaltered, in the proposed DMSC they are full matrices allowing the mode shapes to be changed in a desired set of dof (Serra et al., 2013).

In this system description, the effect of a state observer is not considered and the principal coordinates are assumed to be available for control synthesis. In practice this can be achieved by using modal sensors and, consequently, pre-filtering the worsening observation spillover effects. Even in this case, however, owing to the control spillover, the nm noncontrolled modes excite the m controlled modes, eliminating the desired effect of mode shape imposition.

Therefore, only in the case of distributed sensors and actuators the spillover can be properly canceled, eliminating the coupling elements between the controlled and noncontrolled modes in equations (5). This implies that the controlled modes evolve in a fully independent manner compared with the remaining modes and the controlled poles and mode shapes can be precisely imposed with a proper synthesis of the matrices $\mathbf{G_v}$ and $\mathbf{G_p}$. In these cases it is possible, for example, to create virtual nodes in desired dof of the system in a certain frequency range with significant engineering advantages (Serra et al., 2013).

2.2. Indirect eigenstructure assignment

In many control problems, the availability of sensors and actuators is limited and the control designer cannot always set their positions. Consequently, to make DMSC accessible also in such cases, an alternative indirect version of the methodology has been developed.

This section shows how, even in the presence of discrete sensors and actuators, the use of DMSC makes it possible to take advantage of the full gain matrices, modifying the mode shapes in addition to the controlled poles. In particular, this strategy is able to suppress the vibrations in desired points of the structure and in a determined range of frequencies when the location of external disturbance is known or by estimating the corresponding Lagrange components (Balas, 1978; Cazzulani et al., 2012). This result is achieved by introducing a suitable performance index (PI).

In presence of discrete sensors, a dynamic state observer is necessary to estimate the modal coordinates needed by the controller. By including this in the description above, the closed loop system can be represented by the block diagram shown in Figure 1. Here, we do not report explicitly the standard derivation of state space matrices and vectors, starting from the mechanical description of the system given in equation (5).

In the block scheme, a state space representation of the system is adopted and the dynamic state observer is governed by the equation

$$\begin{cases} \dot{\mathbf{x}}_\mathbf{o} = \mathbf{A_o x_o} + \mathbf{B_{xo} f_c} + \mathbf{K}(\mathbf{y} - \hat{\mathbf{y}}) \\ \hat{\mathbf{y}} = \mathbf{C_o x_o} \end{cases} \tag{9}$$

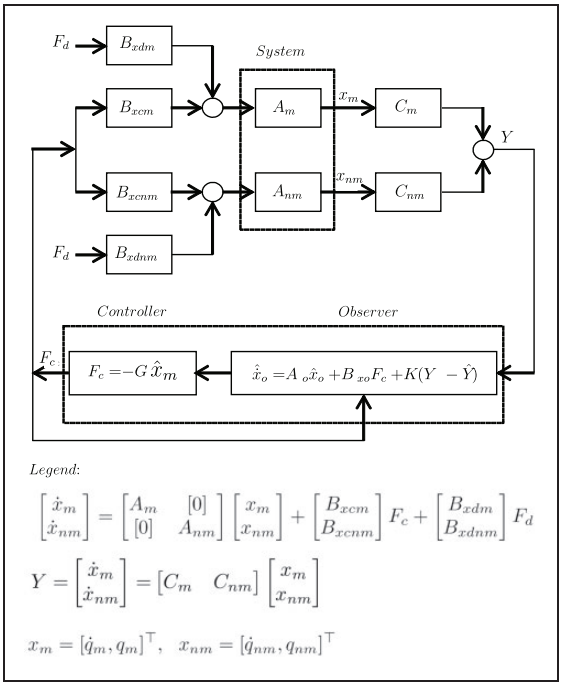

Figure 1. The block scheme of the closed loop system for the DMSC indirect mode shapes imposition logic (in the legend the compact state space form of the system described in equation (5) is reported).

For a number c of controlled modes, the state observer estimates the first o modes, where $c \le o \le m$, and the estimation error dynamics is determined by the observer gain matrix $\mathbf{K}$. It is important to have the observer poles at least twice as fast as the controller poles in order to provide reasonable estimated states to the controller.

The number of estimated modes (o) is different from the number of controlled modes (c) in order to distribute the estimation error on the first o modes, improving the accuracy of the first c modes fed back to the controller. The upper limit for the number of estimated states o is given by the rank of the system's observability matrix, and it depends on the number and locations of the available sensors.

The selected PI to be minimized is the integral of the FRF amplitude between the disturbance and the displacement (Y) of a desired point where vibration suppression is needed

$$PI = \int_{\Omega_{\min}}^{\Omega_{\max}} |FRF|_{F_d \mapsto Y} \mathrm{d}\Omega \tag{10}$$

In the PI, only the FRF absolute value is considered, disregarding the phase because stability is guaranteed by the optimization itself. If vibrations need to be suppressed in more than one point, the performance index is a weighted sum of the single ones. The optimal closed loop mode shapes are selected by using a genetic algorithm (GA)(Deep et al., 2009; Schmitt, 2001) performing a constrained optimization. The frequency range $[\Omega_{\min}, \Omega_{\max}]$ is selected depending on the kind of disturbance exciting the structure and is strictly related to the physical application.

Like in many model-based Active Vibration Controllers (AVCs), in our observed based logic, the optimization procedure considers only the reduced model of order m. The parameter m is selected making a trade-off between the accuracy of the performance index, the stability conditions of the closed loop and the effort needed to identify the parameters.

In short, the application of DMSC in the indirect mode shape imposition can be summarized in six steps:

- selection of the frequency range in which the index should be minimized $[\Omega_{\min} - \Omega_{\max}]$;
- selection of the desired controlled poles (c) of the system in terms of damping ratio ξ and frequency ω;
- selection of the desired observer poles (o) in terms of damping ratio ξ and frequency ω for computing the observer gain matrix $\mathbf{K}$;
- selection of the number of modeled modes (m) on which closed loop stability is ensured, based on the structure modal density;

- optimal set of closed loop mode shapes found by the GA so that the PI is minimum and the stability constraint is satisfied;
- calculation of the $\mathbf{G}_v$ and $\mathbf{G}_p$ gain matrices.

Imposing an input-output relation as the proposed PI, implies that the effect of control and observation spillover are considered in advance for the computation of the controller gains and are not a passive consequence in the closed loop. With the proposed strategy, it is also possible to impose a stability margin for the first m modes requiring their real part to be less than a threshold value in the constrain function. For the technical and detailed description of the control gain synthesis see Serra et al. (2013).

Below is a summary of the main differences between direct and indirect methods listed in terms of Advantages (A) and Drawbacks (D):

1. Direct Method:
   a. A: Direct imposition of the closed loop mode shapes permits the creation of virtual nodes in a desired frequency range. This could be used to cancel the vibration in specific locations of the structure or to cancel the energy input of an external force by nullifying its Lagrange component.
   b. A: The closed loop poles are imposed precisely and will not be affected by spillover effects. This advantage is significant in the case of structures with high modal density such as plates or, in general, light-flexible structures.
   c. A: It allows total redirection of control effort only to the desired location on the structure ensuring at the same time closed loop stability of the modeled modes.
   d. D: Modal sensors and actuators are needed. These are expensive and their position cannot always be chosen by the control designer.
   e. D: Modal sensors and actuators for generic structures do not exist but have to be manufactured and customized.
   f. D: Significant control forces are generally required.

2. Indirect Method:
   a. A: This method permits selection of closed loop poles regardless of mode shape modification.
   b. A: It assigns the optimal set of controlled mode shapes for the desired performance. This allows the control effort to be redirected only to a specific region of the structure.
   c. A: Active compensation of spillover effect for a preselected set of noncontrolled modes. This is a great advantage of DMSC and it is due to the greater dimension of the control parameter space.
   d. A: The differential effect brought about by mode shape modification can be used for example to ensure a closed loop stability margin or to impose a priori maximum allowable control action to avoid saturation of actuators.
   e. D: Significant control forces are generally required.

Finally, in case of nonclassically damped systems, the IMSC could not be applied while our proposed logic, the indirect method in particular, would still keep its validity leading to the minimization of the desired PI.

3. The experimental test rig and the numerical model

This section describes the numerical model and the experimental test rig used to validate the proposed

Table 1. The cantilever beam test rig; geometry and material.

l Length (m)	w Width (m)	t Thickness (m)	E Young's modulus (MPa)	m Unitary length mass (kg/m)
1.0	4.0×10^{-2}	6.1×10^{-3}	67,000	0.754

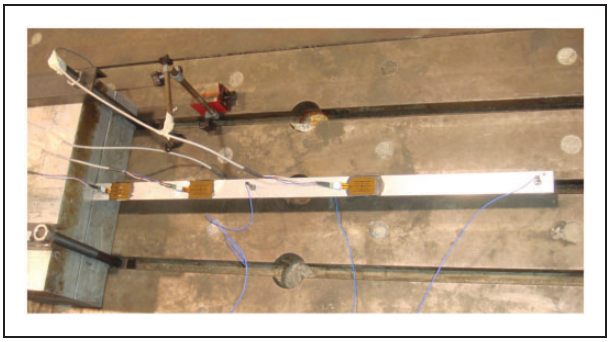

Figure 2. The cantilever beam test rig for the DMSC experimental validation.

Table 2. The cantilever beam test rig; piezoelectric accelerometer positions with respect to the clamp (see Figure 4).

	a_1	a_2	a_3
Position (cm)	40	55	95

logic for indirect mode shapes imposition. The experimental test rig is composed of an aluminum cantilever beam, whose properties are summarized in Table 1, instrumented with three accelerometers and four piezo actuators (three for controlling the structure and one for the external disturbance) as shown in Figure 2.

Table 3. The cantilever beam test rig; piezoelectric actuators positions with respect to the clamp (see Figure 4).

	F_d	F_{c1}	F_{c2}	F_{c3}
Position (cm)	[40–45]	[5–10]	[25–30]	[60–65]

The vibrations are measured by piezoelectric accelerometers *Bruel & Kjaer* 4501*A*, while the control and disturbance actions are provided by piezoelectric patches *Mide QP*20*W* and modeled as equivalent bending moments on the structure. The sensor and actuator positions with respect to the clamp are reported respectively in Tables 2 and 3.

Figure 3 shows a schematic representation of the experimental test rig. The acceleration signals measured on the structure are analogically filtered with a

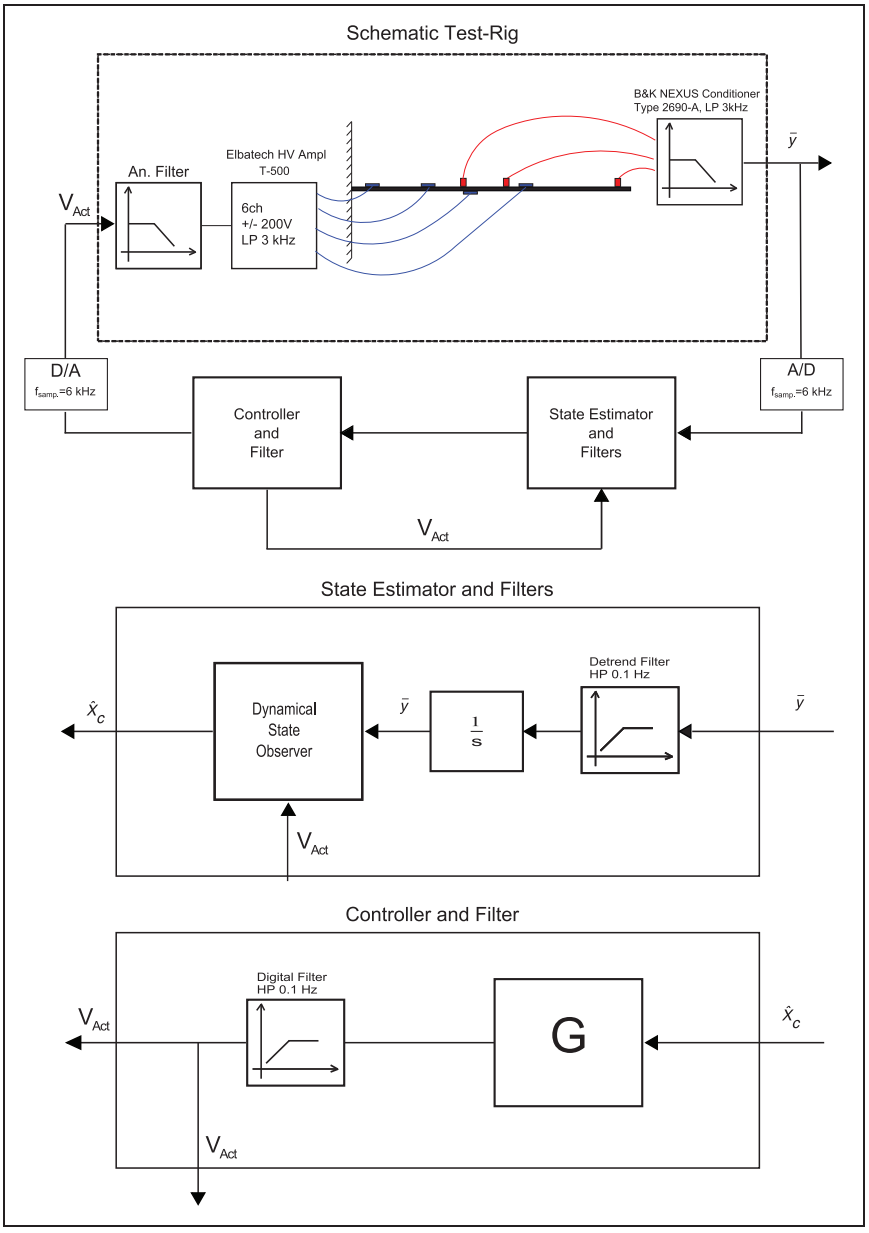

Figure 3. The test rig, the state observer and the controller block scheme.

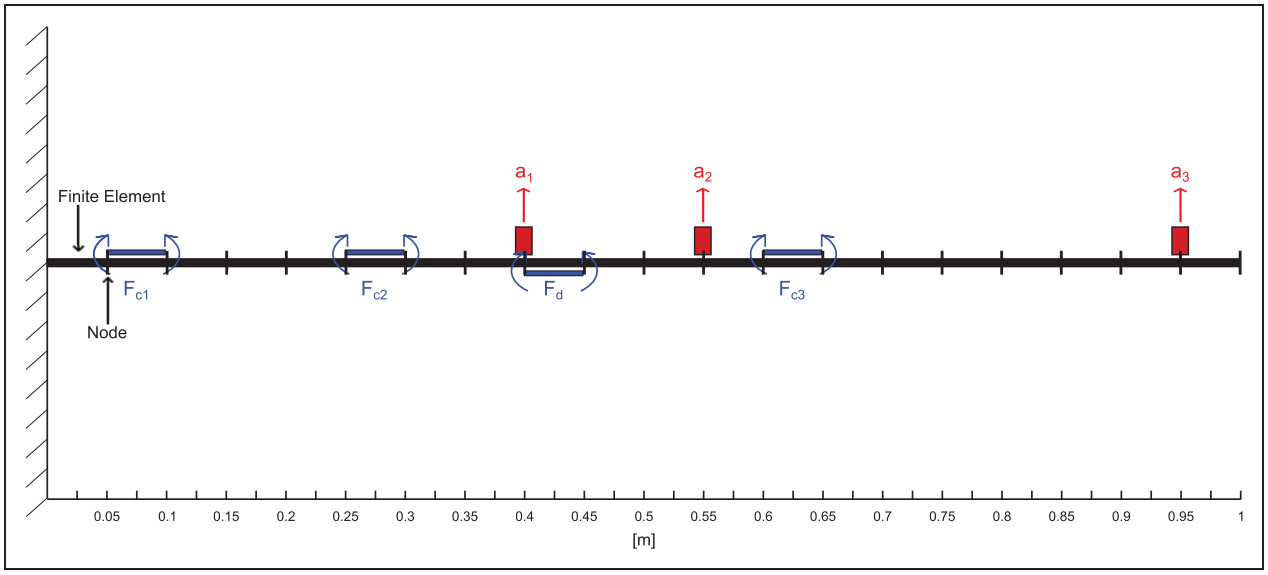

Figure 4. The cantilever beam FEM model for the DMSC validation.

conditioning amplifier to avoid aliasing and then digitalized through the *dSPACE* software-hardware interface. The accelerations are then digitally filtered with a high pass filter (cutoff frequency 0.1 Hz) to delete any low-frequency components mainly due to slightly different ground voltage between the accelerometer conditioner and other instruments in the measuring chain. After that, the signals are integrated to supply the corresponding velocities to the state observer. The first c estimated modes are fed to the controller providing control actions after being further processed by a digital high pass filter to cancel the components at very low frequencies. Finally the control actions are analogically filtered to delete the high frequency contents generated by the D/A conversion and sent to the power amplifier before reaching the actuators on the structure.

A numerical model describing the dynamics of the clamped aluminum beam has been constructed using the FEM approach, also taking into account the inertial (for accelerometers) and stiffness (for piezo-actuators) contributions coming from the instrumentation. The system has 20 mono-dimensional finite elements, 21 nodes (one constrained) with 3 dof per node (axial and vertical displacement and bending rotation) and cubic formulation, resulting in a total of $n = 60$ dof (Figure 4).

In the present study, the target frequency range is $[0 - 100]$ Hz thus, the first three modes contained in this interval are controlled. The first six modes are observed and closed loop stability is ensured for the first eight modes. Regarding the stability margin of the first m modes, apart from the closed loop stability, no further constraints on the real part of the uncontrolled poles are imposed. As already mentioned, while the selection of the number of controlled poles c is strictly linked to the target frequency range, the selection of o and m is system dependent and is done by balancing the effort required by the identification of modal quantities and the desired accuracy of the model. For example, in case of systems with some modes that tend to become unstable because of very low structural damping, it is recommended to set m appropriately ensuring the closed loop stability of those modes.

Table 4. IMSC and DMSC control parameters.

m	o	c	Ω_{min}	Ω_{max}
8	6	3	0 (Hz)	100 (Hz)

In Table 4, the control parameters selected for the present application are summarized.

Since m is the highest mode number, the modal parameters up to the mth principal coordinate should be estimated for numerical model fine tuning. The first eight frequencies and the corresponding damping ratios were identified by different linear sweep tests centered on each eigenfrequency, and are shown in Table 5. The identification process is based on the Prony's method and a multi-step optimization in the frequency domain, as shown in Ripamonti et al. (2014).

After estimating the system's eigenfrequencies and damping ratios, the mode shapes were also estimated. To validate the identification process, a comparison between the numerical and experimental FRF is

shown. For example, in Figure 5, the FRF between the external disturbance and the three accelerations are shown, demonstrating very good agreement between the numerical and experimental FRF.

Slight differences occur in correspondence with the anti-resonances (Figure 5(c)) owing to the lack of the contribution of the higher, nonmodeled modes (Reynders, 2012).

Table 5. First eight uncontrolled poles in terms of eigenfrequencies and damping ratios.

mode n^o	1	2	3	4
ω (Hz)	5.2	31.4	88.4	173.7
ξ%	0.60	0.46	0.31	0.23
mode n^o	5	6	7	8
ω (Hz)	284.8	431.2	594.3	803.4
ξ%	0.30	0.16	0.22	0.24

4. The numerical and experimental comparison between DMSC and IMSC

As stated in the previous section, $[0-100]$ Hz is the frequency range where vibrations need to be suppressed and the selected PI is the unweighted sum of the single PI between the disturbance and the transversal displacements in correspondence with the three sensor positions Y_1, Y_2 and Y_3. In the proposed application, since vibration reduction is required in a relative low-frequency range, displacement terms are considered in the PI. If control needs to act at higher frequencies, e.g. for noise reduction, the FRF in the PI could be expressed in terms of accelerations, enhancing the effects on the higher modes. In Tables 6 and 7, the controller and the observer poles are reported in terms of frequency and damping ratio.

After imposition of the poles needed for the control algorithm, the performance of the state observer in open loop has been checked, comparing the numerical

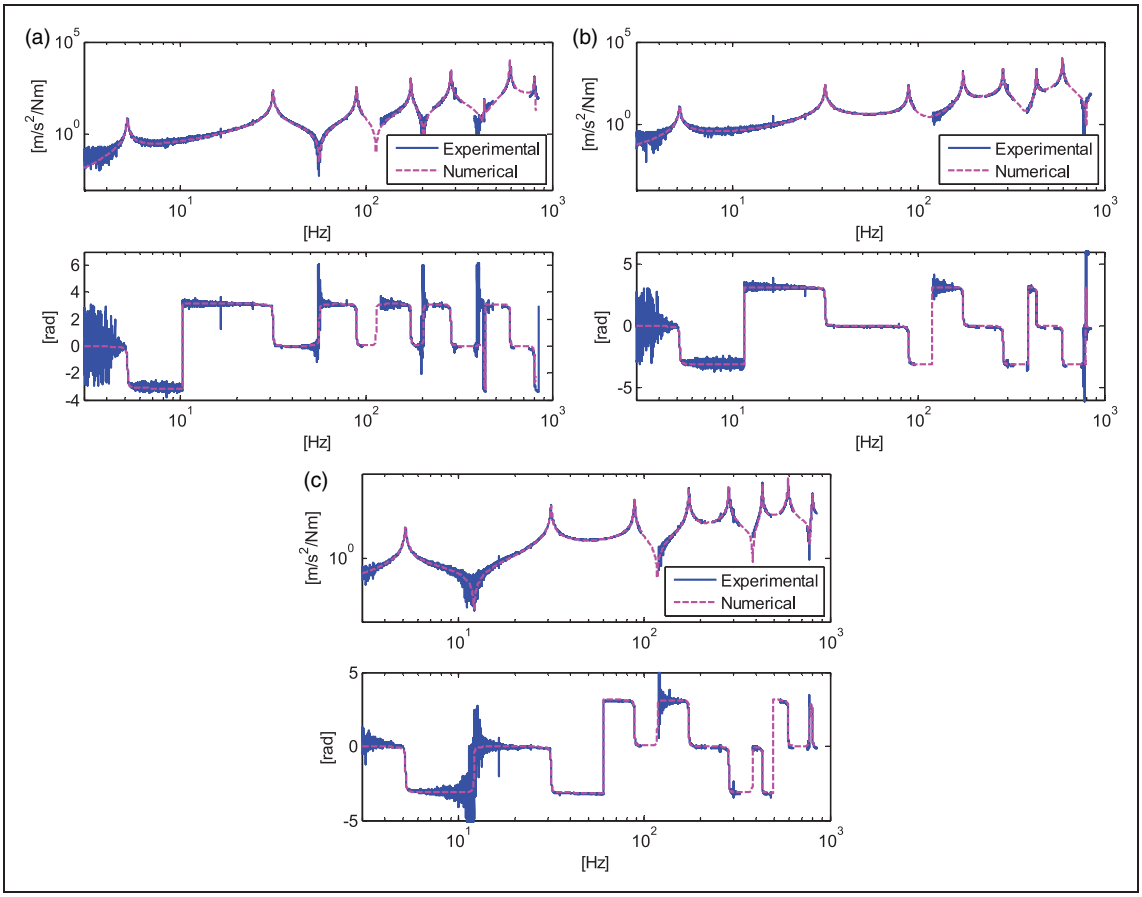

Figure 5. The cantilever beam numerical-experimental comparison; FRF a_1/F_d (a), FRF a_2/F_d (b) and FRF a_3/F_d (c) for the uncontrolled system (open loop).

Table 6. Imposed controlled poles both for the IMSC and the DMSC.

mode n^o	1	2	3
ω_c (Hz)	5.2	31.4	88.4
ξ_c %	9.0	7.0	3.5

Table 7. Imposed observer poles both for the IMSC and the DMSC.

mode n^o	1	2	3	4	5	6
ω_o (Hz)	5.2	31.4	88.4	173.7	284.8	431.2
ξ_o %	30	30	30	30	30	30

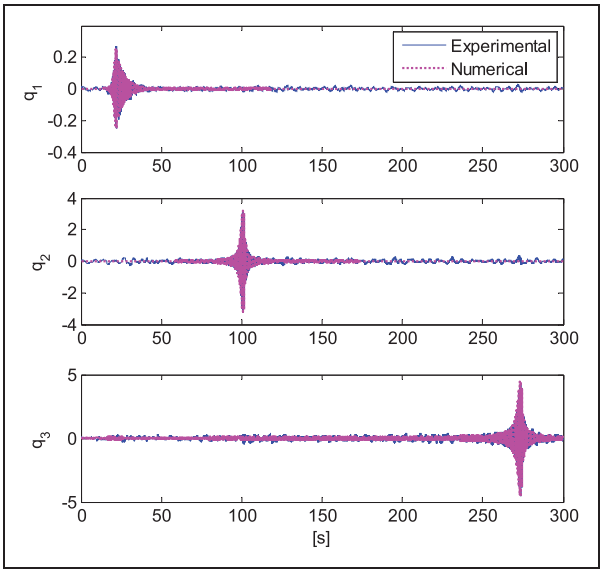

Figure 6. The cantilever beam numerical-experimental comparison; the first three modal coordinates estimated by the observer in open loop.

and experimental estimates of the principal coordinates fed to the controller (Figure 6).

Exciting the system with sweep forcing ($\Omega_{\min} = 0$, $\Omega_{\max} = 100$ Hz and $\Delta\Omega = 0.33$ Hz/s), it is possible to see how the observer is able to decouple the principal coordinates proving again a good numerical-experimental match.

In Figure 7, the experimental FRF between the disturbance and the transversal displacements Y_i are shown for the uncontrolled and controlled systems (both with IMSC and DMSC).

It is important to underline that the assigned controller and observer poles are the same for IMSC and DMSC, and the differential effect is due only to mode shape modification. In correspondence with the first output, the vibration reduction achieved by DMSC is smaller than those in the other outputs. This is because the first output location is closer to the clamp and has an intrinsically lower weight in the global PI compared with the others.

In Figure 8, the uncontrolled and the modified mode shapes are shown. Since the modal coordinates are unaltered, even a simple gain and/or sign modification of the mode shape would lead to sensible effects in the system response. As broadly explained in Serra et al. (2013), the controlled mode shapes shown in Figure 8 are a linear combination of the first three uncontrolled modes without considering the spillover contributions coming from the others. The mode shapes for the DMSC controlled system, estimated from the experimental data at the measure points (accelerometers), have been represented by the green squares.

In order to show the effectiveness of the method, a time domain analysis has also been carried out. In particular, the responses to a random disturbance in correspondence with the three outputs are shown in Figure 9 for uncontrolled and controlled systems with both DMSC and IMSC. A random disturbance bending moment of 0.2 Nm amplitude with constant spectrum in the frequency range $[0.1 - 100]$ Hz is applied.

Given the time responses of the system in correspondence with the three outputs, it is possible to compute the RMS values of each signal and quantitatively compare the performance achieved with the two different control strategies (Table 8).

These results confirm what is already shown in the FRF plots: the proposed control strategy is able to redirect the control effort in a specific location on the structure through a proper selection of the PI.

In order to prove the reliability of the model also in closed loop, a numerical experimental comparison of both the IMSC and DMSC system is shown in Figure 10. As an example, the FRF between the disturbance and the third output is shown. The good closed loop numerical-experimental match is achieved thanks to the choice of the parameter m. Picking it closer to c would lead to a bigger mismatch because the spillover effects of the first $(m - c)$ nonmodeled modes would not be included in the model. For the DMSC, in Figure 10(b), the numerical-experimental match is slightly worse than the one obtained with the IMSC, in Figure 10(a). This difference mainly arises at the anti-resonances, where the signal-to-noise ratio is low and the lack of nonmodeled modes is more evident (Reynders, 2012), as previously discussed.

Finally, some considerations can be made on the control energy used by the two logics. In Table 9 a comparison in terms of control action RMS (calculated

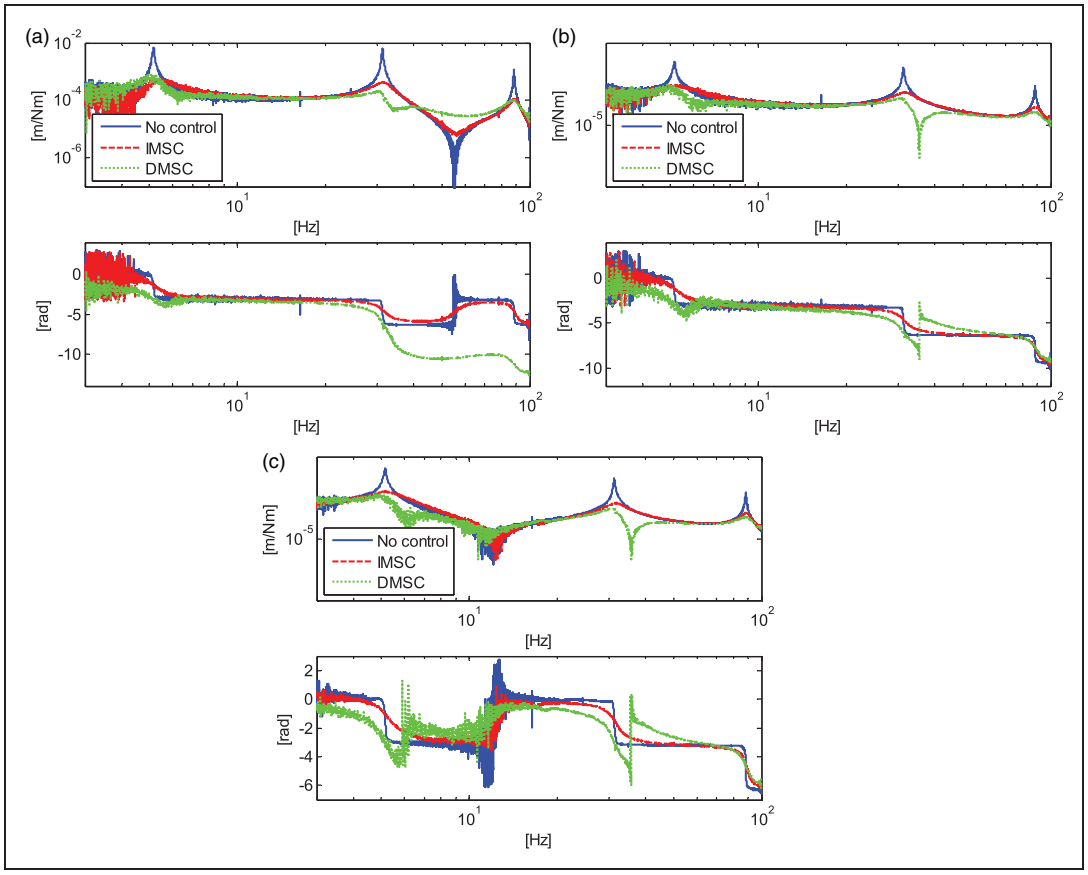

Figure 7. The cantilever beam experimental test; FRF Y_1/F_d (a), FRF Y_2/F_d (b) and FRF Y_3/F_d (c) for the uncontrolled system, the IMSC and the DMSC.

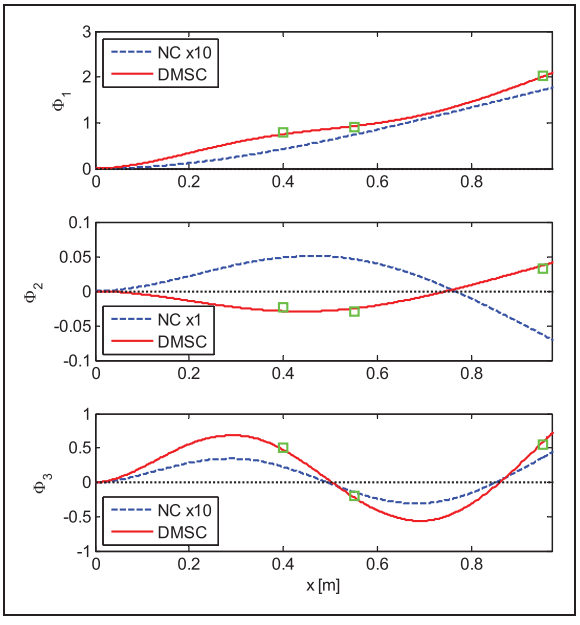

Figure 8. The cantilever beam mode shapes comparison; the first three mode shapes for the uncontrolled (NC) and the DMSC controlled system. (In order to allow the comparison, mode 1 and 3 have been $\times 10$ amplified).

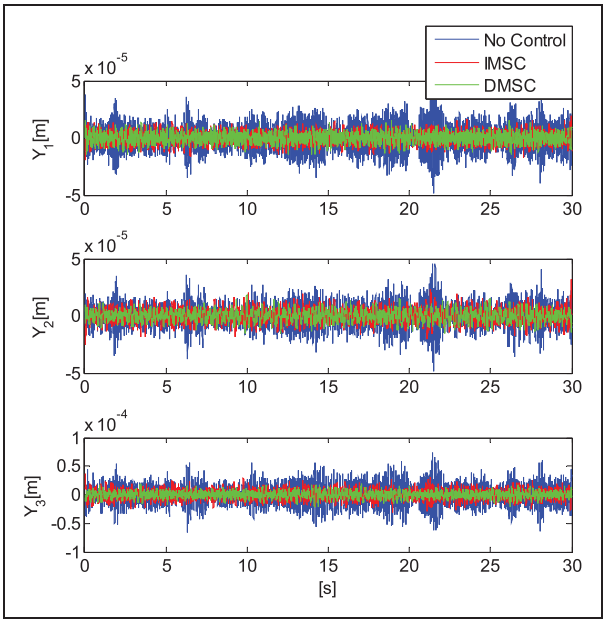

Figure 9. The cantilever beam experimental test; time histories of the system response (Y_1, Y_2 and Y_3) to a random disturbance for the uncontrolled system, the IMSC and the DMSC.

during the random disturbance test and normalized with respect to the actuator full-scale) is shown for each piezoelectric patch.

It is well-known that modifying the mode shapes requires higher control effort than simple modification of the system's poles. However, changing only the poles of the system cannot create vibration nodes. This implies that, even reaching the saturation limit of actuators, DMSC performance would not be achievable using IMSC.

This constraint has to be considered by the control designer. If control action needs to be limited within given thresholds, it is possible to include this either in the constraint function or by adding a penalty term in the PI, e.g. limiting the H_∞ norm of the FRF between the disturbance and the control forces.

5. Conclusions

This paper shows the numerical and experimental validation of a recently developed control strategy based on a modal approach and called Dependent Modal Space Control (DMSC). The proposed logic is designed to impose both the closed loop poles and mode shapes. The latter, from an engineering point of view, could permit, for example, the creation of virtual nodes to enhance control performance. DMSC is able to redirect the control effort to desired and concentrated locations of the structure and reduce vibrations in a desired frequency range. A main difference with respect to many other control logics is that DMSC can ensure closed loop stability on a desired number of modeled controlled and noncontrolled modes in a generic non co-located configuration. Furthermore, the annoying spillover contribution is considered a priori in controller synthesis and not passively as a side effect.

The closed loop eigenvalues and corresponding eigenmodes are imposed independently in the control logic. This means that the closed loop poles of the system are defined and then the optimal set of mode shapes to minimize the selected PI is computed. Owing to the modification of the mode shapes, the control forces required by DMSC are generally higher than those required by IMSC. If certain thresholds must not be exceeded, this can be included in the control synthesis. The algorithm structure also makes it possible to require a threshold stability margin for all the modeled modes.

Table 8. The cantilever beam test rig; RMS % improvement between the uncontrolled system (NC) the IMSC and the DMSC during the random disturbance test.

Output	Y_1	Y_2	Y_3
Improvement % IMSC-NC	73	73	75
Improvement % DMSC-NC	75	82	81
Improvement % DMSC-IMSC	7	32	24

Table 9. The cantilever beam test rig; comparison between the control effort RMS (normalized with respect to the actuator full scale) for the IMSC and the DMSC controlled systems during the random disturbance test.

Control effort	Fc_1	Fc_2	Fc_3
IMSC RMS %	2.1	2.1	4.2
DMSC RMS %	14.2	20.5	20.0

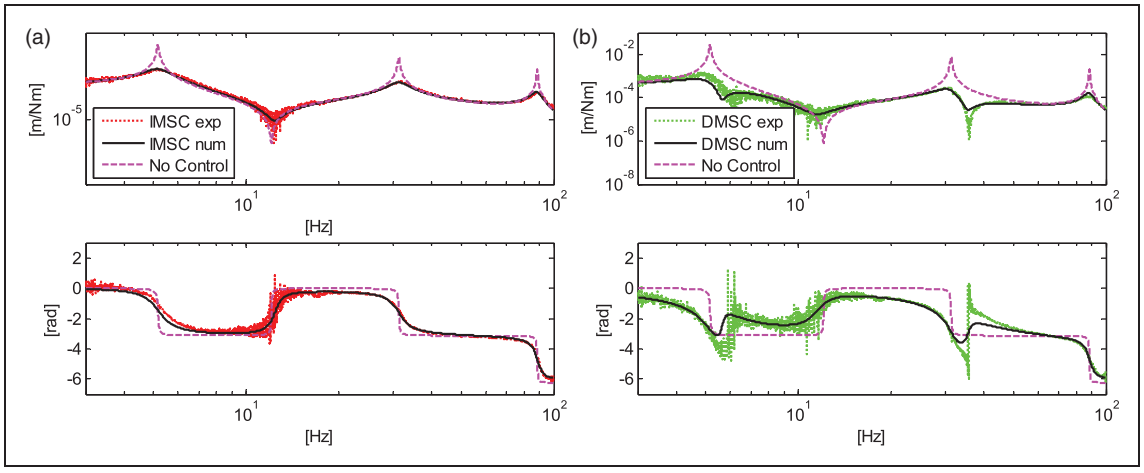

Figure 10. The cantilever beam numerical-experimental comparison; FRF Y_3/F_d for the uncontrolled system, the IMSC (a) and the DMSC (b).

The proposed method has been tested in numerical and experimental simulations on a cantilever beam, demonstrating the advantages of DMSC with respect to the classic IMSC and underlining the differential effects due to mode shape modification. In particular, with the same closed loop poles, the differential effect given by mode shape modifications improved vibration reduction by approximately 20%. A good numerical-experimental match was also demonstrated both in open and in closed loop.

Finally, this work is intended as a conceptual proof of the proposed control logic; further applications on more complex structures, such as a long-span bridge aeroelastic model for wind tunnel tests, are currently in progress.

Funding

This research received no specific grant from any funding agency in the public, commercial, or not-for-profit sectors.

References

Bagordo G, Cazzulani G, Resta F, et al. (2011) A modal disturbance estimator for vibration suppression in non-linear flexible structures. *Journal of Sound and Vibration* 330(25): 6061–6069.

Balas MJ (1978) Active control of flexible systems. *Journal of Optimization theory and Applications* 25(3): 415–436.

Baz A and Poh S (1990) Experimental implementation of the modified independent modal space control method. *Journal of Sound and Vibration* 139(1): 133–149.

Cazzulani G, Resta F and Ripamonti F (2012) Vibration reduction on a nonlinear flexible structure through resonant control and disturbance estimator. Proceedings of SPIE. *The International Society for Optical Engineering*, 8341, art. no. 83411H, San Diego, USA.

Chandrashekhara K and Agarwal A (1993) Active vibration control of laminated composite plates using piezoelectric devices: A finite element approach. *Journal of Intelligent Material Systems and Structures* 4(4): 496–508.

Deep K, Singh KP, Kansal M, et al. (2009) A real coded genetic algorithm for solving integer and mixed integer optimization problems. *Applied Mathematics and Computation* 212(2): 505–518.

Fang J, Li Q and Jeary A (2003) Modified independent modal space control of mdof systems. *Journal of Sound and Vibration* 261(3): 421–441.

Fuller CR, Snyder S, Hansen C, et al. (1992) Active control of interior noise in model aircraft fuselages using piezoceramic actuators. *AIAA journal* 30(11): 2613–2617.

Kim MH and Inman DJ (2001) Reduction of observation spillover in vibration suppression using a sliding mode observer. *Journal of Vibration and Control* 7(7): 1087–1105.

Klein G and Moore B (1977) Eigenvalue-generalized eigenvector assignment with state feedback. *Automatic Control, IEEE Transactions on* 22(1): 140–141.

Liu GP and Patton RJ (1998) Low sensitive and robust control design via output feedback eigenstructure assignment. *IEE Conference Publication* (455): 457-462.

Meirovitch L and Baruh H (1985) The implementation of modal filters for control of structures. *Journal of Guidance, Control, and Dynamics* 8(6): 707–716.

Meirovitch L, Baruh H and OZ H (1983) A comparison of control techniques for large flexible systems. *Journal of Guidance, Control, and Dynamics* 6(4): 302–310.

Mottershead JE, Tehrani MG, James S, et al. (2008) Active vibration suppression by pole-zero placement using measured receptances. *Journal of Sound and Vibration* 311(3): 1391–1408.

Qiu Zc, Zhang Xm, Wu Hx, et al. (2007) Optimal placement and active vibration control for piezoelectric smart flexible cantilever plate. *Journal of Sound and Vibration* 301(3): 521–543.

Resta F, Ripamonti F, Cazzulani G, et al. (2010) Independent modal control for nonlinear flexible structures: An experimental test rig. *Journal of Sound and Vibration* 329(8): 961–972.

Reynders E (2012) System identification methods for (operational) modal analysis: Review and comparison. *Archives of Computational Methods in Engineering* 19(1): 51–124.

Ripamonti F, Leo E and Resta F (2014) A comparison between non linear control logics applied to a 3-segments manipulator. *Proceedings of SPIE – The International Society for Optical Engineering*, 9057, art. no. 90572K, San Diego, USA.

Schmitt LM (2001) Theory of genetic algorithms. *Theoretical Computer Science* 259(1): 1–61.

Serra M, Resta F and Ripamonti F (2013) Dependent modal space control. *Smart Materials and Structures* 22(10): 105004.

Singh S, Pruthi HS and Agarwal V (2003) Efficient modal control strategies for active control of vibrations. *Journal of Sound and Vibration* 262(3): 563–575.